ELSEVIER

Journal of Nuclear Materials 313–316 (2003) 1277–1281

journal of nuclear materials

www.elsevier.com/locate/jnucmat

Simulation of divertor detachment characteristics in JT-60 with superconducting coils

K. Shimizu *, T. Takizuka, S. Sakurai, H. Tamai, H. Takenaga, H. Kubo, Y. Miura

Japan Atomic Energy Research Institute, Naka-machi, Naka-gun, Ibaraki-ken 311-0193, Japan

Abstract

The capability of detachment control in JT-60SC is demonstrated with a divertor code (SOLDOR/NEUT2D). Under the standard operation of the core edge density at 95% of the minor radius, $n_{edge} = 3.2 \times 10^{19}$ m^{-3}, the power flow from the core plasma $Q_e = Q_i = 6$ MW, and the conductance of inner and outer cryopanels $C_{in} = C_{out} = 50$ m^3/s, the inner divertor plasma is partially detached and the outer divertor plasma attached. The inner divertor can be changed from partially detached to attached plasma by inner pump of 150 m^3/s. The fully detached inner divertor is obtained in high density operation with $n_{sep} > 4 \times 10^{19}$ m^{-3}, where n_{sep} is the density at the separatrix outer midplane, The elastic collision in a dense and cold divertor plasma ($n_e \geqslant 5 \times 10^{20}$ m^{-3}, $T_e < 5$ eV) play an important role on detachment.

PACS: 52.65.Kj

Keywords: Divertor; Simulation; JT-60SC; Elastic collision; Detachment; Monte Carlo

1. Introduction

JT-60 has a plan to modify the machine to a superconducting coil tokamak, JT-60SC [1] to establish scientific and technological bases for an attractive DEMO reactor. The main objectives of the divertor research in JT-60SC is to demonstrate detachment control under the condition of a radiation fraction of ~90%. In order to control detachment and reduce impurity contamination in the main plasma with SOL flow induced by gas puffing and divertor pumping, two cryopanels are installed under the private dome and an outer divertor. Fig. 1 shows the JT-60SC divertor configuration. The designed pumping speed of each cryopanel is 200 m^3/s. The divertor characteristics of JT-60SC have been investigated using a 2D divertor code (SOLDOR/NEUT2D) [2]. The purpose of this paper is to investigate the capability of pumping and gas puffing of controlling the detachment of divertor plasma. In the dense and cold divertor plasma, elastic collision becomes important. Its effect on the divertor detachment is also examined. The simulation model is described in Section 2. The simulation results for the JT-60SC divertor characteristics are presented in Section 3. Summary is given in Section 4.

2. Simulation code

The plasma parameters are calculated with a 2D fluid code SOLDOR coupled with a 2D Monte Carlo neutral code, NEUT2D. The model equations used in the SOLDOR code are identical to the B2-code [3]. Fluid equations are discretized in space by a finite volume method and are full implicitly discretized in time, where terms i.e. parallel/perpendicular diffusion and convective terms are evaluated at the next step ($t = t^{N+1}$). Furthermore, the terms at t^{N+1} are linearized by the

* Corresponding author. Tel.: +81-29 270 7747; fax: +81-29 270 7468.

E-mail address: kshimizu@naka.jaeri.go.jp (K. Shimizu).

0022-3115/03/$ - see front matter
PII: S0022-3115(02)01494-0

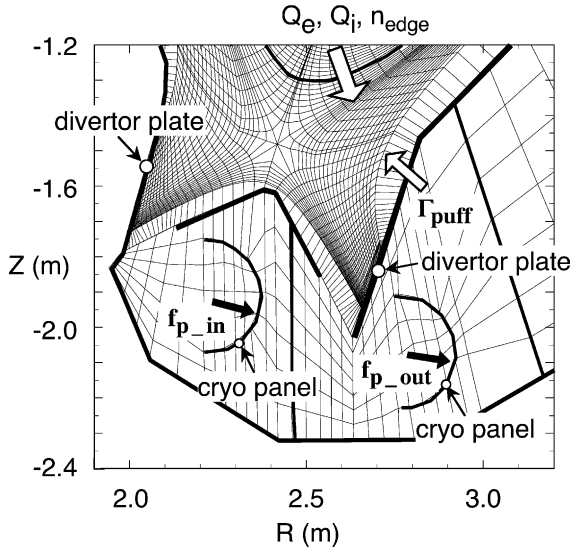

Fig. 1. JT-60SC divertor configuration. Two cryopanels are installed under the private dome and the outer divertor. The grid used in simulations, the boundary condition (the electron density at the core edge n_{edge}, the electron power flow Q_e, the ion power flow Q_i), the gas puffing rate from outer board Γ_{puff}, the exhaust probability (When neutral particles hit cryopanels, they are exhausted with this probability.) f_p are also shown.

Newton–Raphson method. The discretized equations are solved efficiently using approximate factorization method. The feature of our code is that the total variation diminishing (TVD) scheme [4] is applied for convective terms, for example $\nabla \cdot (n_i \mathbf{v}_{\|i})$ in the ion particle conservation equation. The TVD schemes carefully treat dissipation to get a solution without numerical oscillation and can simulate a shock wave without a deformation of shock front. A simple radiation model is employed, where a fraction of carbon impurity is assumed to be 1.0% of the deuterium density and the radiation loss coefficient $L_z(T_e)$ is enhanced by impurity recycling effect with assuming $n_e \tau_{recycle} = 10^{16}$ s m^{-3} [5].

The neutral gas transport is solved with a Monte Carlo code, where test particles are followed by the path-length estimator method. The code treats the recycling neutral at the divertor plates and the wall, gas puffing and the volume recombination (RC). Under the dense and cold divertor conditions elastic collisions between neutrals and plasma ions become important. Therefore, the elastic collision model is incorporated into the NEUT2D code. The model, which is similar to the DEGAS 2 code [6], simulate the elastic collision as follows:

(1) The collision point of neutral test particles is calculated from $\int_0^L \mathrm{d}s/\lambda(s) = -\ln \xi$ where L is the free flight length, s is the distance from the emitted point or the previous collision point along a straight line, ξ is a uniform random number, λ is the local mean free path for all collision processes. i.e. ionization by electrons (I-e), dissociation (DS), charge exchange (CX) and elastic collision (EL).
(2) When a collision occurs, the collision type is chosen in accordance with its probability.
(3) When an elastic collision is chosen, an ion collision-partner with a velocity $\mathbf{v}_i$ is sampled from a Maxwellian distribution.
    If $\sigma_{EL}(v_r) \cdot v_r > \xi \cdot [\sigma_{EL}(v_r) \cdot v_r]_{max}$ (where $v_r = |\mathbf{v}_0 - \mathbf{v}_i|$, ξ is a uniform random number), it is rejected, and new velocity is sampled (rejection technique) [6].
(4) The scattering angle θ is sampled from the tables of $\theta(E_r, \xi)$ where E_r is the relative energy and ξ is a uniform random number.
(5) The velocity of test particles after collision is determined from the scattering angle θ and azimuthal angle $\phi = 2\pi\xi$ sampled from a uniform random number.
(6) The test particles are traced until it is absorbed by pumps or is ionized in plasma.

The momentum and energy source terms due to elastic collision are calculated by a kinetic description [7], where they are averaged over the Maxwellian distribution function of the background ions, with following trajectory of test particles.

3. Simulation results

Simulations are carried out mainly under the condition of the density at the core edge (95% of the minor radius), $n_{edge} = 3.2 \times 10^{19}$ m^{-3} and the power flow into the SOL $Q_e = Q_i = 6$ MW. The mesh used in the present simulations is shown in Fig. 1. The pumping effect is simulated by exhausting neutral particles with a probability (f_p) when they hit cryopanels. The particle exhaust probabilities are set to be $f_{p\_in} = 0.021$, $f_{p\_out} = 0.016$, which correspond to effective pumping speed at cryopanels of inner and outer divertor $C_{in} \approx 50$ m^3/s, $C_{out} \approx 50$ m^3/s, respectively. We assume $D_\perp = 0.25$ m^2/s for the particle diffusion coefficient and $\chi_\perp^i = \chi_\perp^e = 1$ m^2/s for the perpendicular thermal diffusivity, which are chosen based on the transport coefficients obtained from simulations for various tokamaks [8]. The classical expressions are used for the transport along the magnetic field. Flux limits for electron heat conduction and momentum flow are used [9]. Fig. 2 shows the density (n_{ed}) and electron temperature (T_{ed}) profiles in front of the target plates. The electron temperatures at the inner and outer strike point are 3.3 and 6.2 eV, respectively. The detachment is characterized by two features: (1) ionization front moves upstream from the vicinity of the targets due to low electron temperature insufficient to ionize

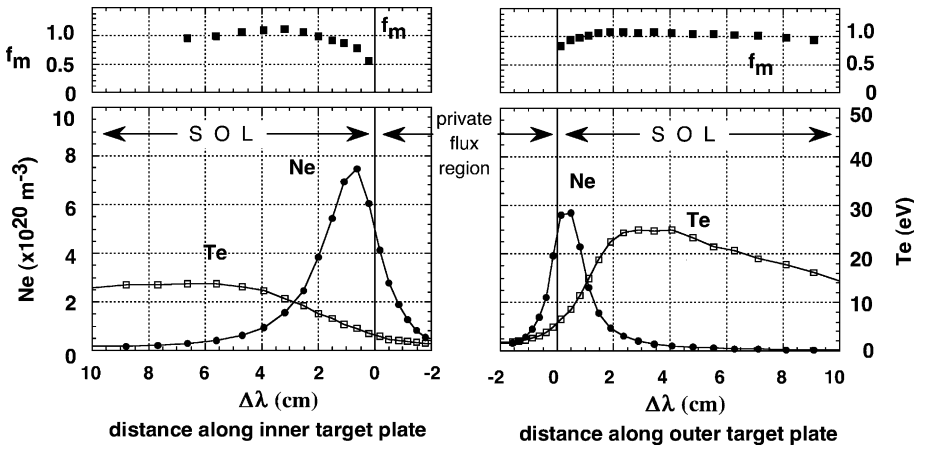

Fig. 2. Radial profiles of electron density and electron temperature in front of the target plates. Closed square shows effective pressure ratio f_m (see text). The simulation parameters are $n_{edge} = 3.2 \times 10^{19}$ m^{-3}, $Q_e = Q_i = 6$ MW, $C_{in} = C_{out} = 50$ m^3/s.

neutral particle (typically ~5 eV); (2) a reduction of plasma pressure due to momentum loss by charge exchange process and elastic collision. For the second feature, we introduce an effective pressure ratio in each flux tube defined as follows:

$$f_m = (p_e + p_i + n_i m_i v_{\|i}^2)_{target} / (p_e + p_i + n_i m_i v_{\|i}^2)_{midplane}. \quad (1)$$

The effective pressure ratio is nearly 1, when the divertor plasma is attached. For the detachment, it falls to $f_m \leqslant 0.5$–0.6 at least. Only f_m value of the flux tube close to the inner strike point is less than 0.6, as shown in Fig. 2. The figure indicates that the inner divertor plasma is partially detached from the target and the outer divertor plasma is attached.

We investigate the requirement for pumping and gas puffing to change the detached/attached condition. The inner strike point becomes attached when the conductance of inner cryopanel is increased from 50 to 150 m^3/s. Fig. 3 shows the density, electron temperature and the effective pressure ratio in front of the inner divertor plate. The parameters of (n_{ed}, T_{ed}, f_m) at the strike point change from (6.3×10^{20} m^{-3}, 3.3 eV, 0.55) to (5.3×10^{20} m^{-3}, 6.7 eV, 0.83). Introducing gas puffing from outboard, the temperature at the outer strike point

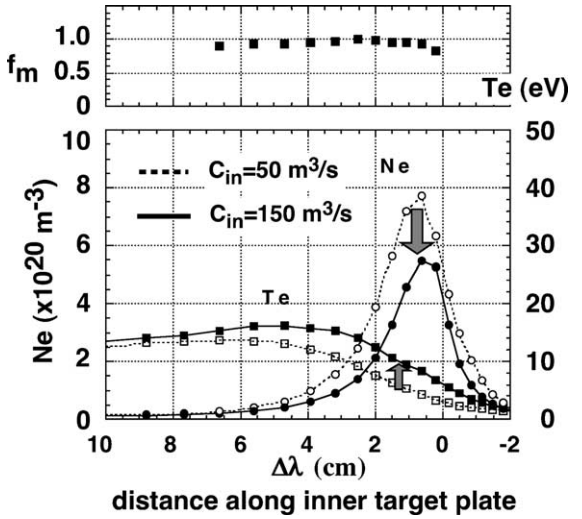

Fig. 3. Radial profiles of electron density and electron temperature in front of the inner target plate. The pumping speed of inner cryopanel is increased from $C_{in} = 50$ m^3/s (broken line) to $C_{in} = 150$ m^3/s (solid line). Closed square shows effective pressure ratio f_m in case of $C_{in} = 150$ m^3/s.

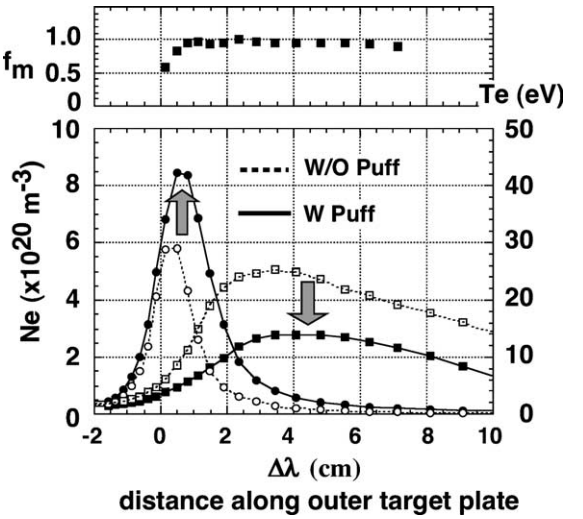

Fig. 4. Radial profiles of electron density and electron temperature without gas puffing (broken line) and with gas puff of $F_{puff} = 0.8 \times 10^{22}$ s^{-1} as a function of distance along outer target plate. Closed square shows effective pressure ratio f_m in case of gas puffing.

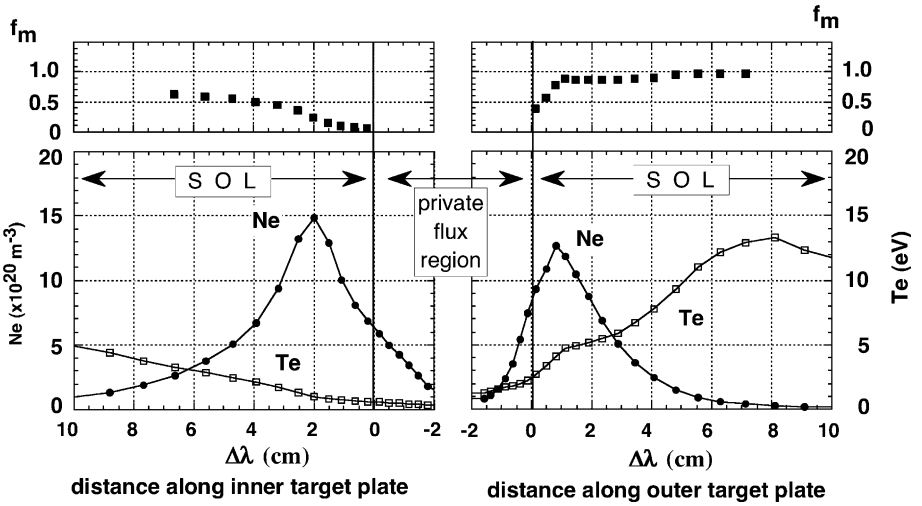

Fig. 5. Radial profiles of electron density and electron temperature in front of the inner and outer target plate in high density operation with $n_{sep} = 4.3 \times 10^{19}$ m^{-3}. Effective pressure ratio f_m indicates the inner divertor is fully detached.

decreases. The outer divertor plasma becomes partially detached at $F_{puff} = 0.8 \times 10^{22}$ s^{-1}. This gas puffing rate correspond to 80% of the particle outflux from the main plasma. The parameters of (n_{ed}, T_{ed}, f_m) at the outer divertor plate are shown in Fig. 4. The parameters at the outer strike point change from (5.8×10^{20} m^{-3}, 6.2 eV, 0.83) to (6.8×10^{20} m^{-3}, 3.8 eV, 0.58).

A series of simulations is carried out for a density scan. When the density at the separatrix reaches $n_{sep} = 4 \times 10^{19}$ m^{-3}, the inner divertor plasma becomes fully detached as shown in Fig. 5. The position of peak target density moves from the inner strike point to 2 cm outside and the peak density reaches 15×10^{20} m^{-3}. The elastic collision effect on the detachment is investigated. Fig. 6 shows the particle flux (F_{id}) onto the inner divertor plate as a function of n_{sep}. Without the elastic collision, the F_{id} increases with separatrix density. On the other hand, the F_{id} calculated with the elastic collision deviates from a linear rise above $n_{sep} \geqslant 3 \times 10^{19}$ m^{-3}. The flux F_{id} decreases above $n_{sep} > 4 \times 10^{19}$ m^{-3} because the density in front of the target decreases due to strong recombination.

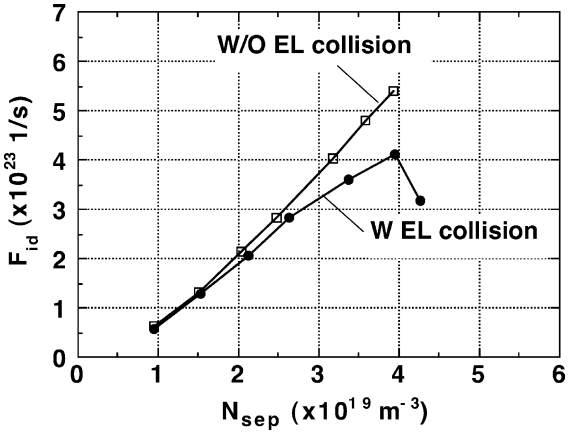

Fig. 6. Particle flux onto the inner target plate calculated with elastic collisions (closed circles) and without elastic collisions (open squares) as a function of the electron density at the midplane. Simulation parameters are the same as those of Fig. 2 except for n_{edge}.

Table 1
Integration of momentum source for each collision type in the inner divertor, which are calculated for the partially detached plasma with $n_{sep} = 3.3 \times 10^{19}$ m^{-3} and elastic collision effects (see Fig. 6)

	Whole region Vol = 0.938 m^3	$T_e < 10$ eV Vol = 0.081 m^3	$T_e < 5$ eV Vol = 0.012 m^3	$T_e < 2$ eV Vol = 0.0002 m^3
I-e	+5.82	+3.61	+42.71	+0.04
CX	−8.42	−7.87	−6.40	−0.07
RC	−0.03	−0.03	−0.03	−0.008
EL-a	−13.65	−12.87	−11.24	−0.83
EL-m	−3.57	−3.57	−3.52	−0.85
Total	−19.85 N	−20.72 N	−18.48 N	−1.72 N

Table 1 shows the integration of the momentum source for each collision type in the inner divertor. They are calculated for the partially detached plasma with $n_{sep} = 3.3 \times 10^{19}$ m^{-3} and elastic collision effects (see Fig. 6). The symbols of RC, EL_a and EL_m stand for recombination ($e + D^+ \rightarrow D$), atomic-elastic collision ($D^+ + D \rightarrow D^+ + D$) and molecular-elastic collision ($D^+ + D_2 \rightarrow D^+ + D_2$), respectively. The symbol of Vol denotes volume. The region where $T_e < 2$ eV is very small so that the momentum source due to recombination is negligible. Table 1 indicates that the dominant mechanism for momentum loss in partially detached plasma is atomic-elastic collision (not charge exchange process).

4. Summary

The divertor characteristics in JT-60SC are investigated with the SOLDOR/NEUT2D code. The capability of detachment control in JT-60SC is demonstrated. Under the standard operation of the edge density $n_{edge} = 3.2 \times 10^{19}$ m^{-3}, the power flow from the core plasma $Q_e = Q_i = 6$ MW, and the conductance of inner and outer cryopanels $C_{in} = C_{out} = 50$ m^3/s, the inner divertor plasma is partially detached and the outer divertor plasma attached. The inner divertor can be changed from partially detached to attached plasma by inner pump of 150 m^3/s. The outer divertor can be changed from attached to partially detached by gas puffing of 0.8×10^{22} s^{-1}, which correspond to 80% of the particle outflux from the main plasma. The fully detached inner divertor is obtained in high density operation with $n_{sep} > 4 \times 10^{19}$ m^{-3}. The elastic collision in a dense and cold divertor plasma ($n_e \geqslant 5 \times 10^{20}$ m^{-3}, $T_e < 5$ eV) play an important role on detachment.

Acknowledgements

The authors wish to thank Drs M. Shimada, A. Sakasai and M. Matsukawa for useful discussions and encouragement.

References

[1] A. Sakasai et al., in: Proc. of 19th SOFE, Atlantic City, USA, 2002.
[2] K. Shimizu, T. Takizuka, T. Hirayama, in: 41st Annual Meeting of APS, Seattle, 1999.
[3] B.J. Brams, Thesis, University of Utrecht, 1986.
[4] S.R. Chakravarthy et al., in: AIAA 86-0243, AIAA 24th Aerospace Science Meeting, 1986.
[5] D.E. Post, J. Nucl. Mater. 220–222 (1995) 143.
[6] R.J. Kanzleiter, D.P. Stotler, et al., Phys. Plasmas 7 (2000) 5064.
[7] P. Bachmann, D. Reiter, Contribution Plasma Phys. 35 (1995) 45.
[8] ITER Physics Expert Group on Divertor, Nucl. Fusion 39 (1999) 2391.
[9] L. Spitzer, R. Harm, Phys. Rev. 89 (1953) 977.